Sorting nexin-1 defines an early phase of *Salmonella*-containing vacuole-remodeling during *Salmonella* infection

Miriam V. Bujny[1,*], Phil A. Ewels[1], Suzanne Humphrey[2], Naomi Attar[1], Mark A. Jepson[2] and Peter J. Cullen[1,‡]

[1]Henry Wellcome Integrated Signalling Laboratories, Department of Biochemistry, School of Medical Sciences, University of Bristol, Bristol, BS8 1TD, UK
[2]Department of Biochemistry, School of Medical Sciences, University of Bristol, Bristol, BS8 1TD, UK
*Present address: Department of Chemistry and Chemical Biology, Harvard University, Cambridge, MA, USA
‡Author for correspondence (e-mail: Pete.Cullen@bris.ac.uk)

Accepted 3 April 2008
Journal of Cell Science 121, 2027-2036 Published by The Company of Biologists 2008
doi:10.1242/jcs.018432

Summary

***Salmonella enterica* serovar Typhimurium replicate within host cells in a specialized membrane-bound compartment, the *Salmonella*-containing vacuole (SCV). Interaction of SCVs with the host endocytic network is modulated by bacterial effectors, some of which, such as SigD/SopB, manipulate the level of endosomal phosphoinositides. Here, we establish that at early stages of *Salmonella* infection, sorting nexin-1 (SNX1) – a host phosphoinositide-binding protein that normally associates with early endosomes and regulates transport to the *trans*-Golgi network (TGN) – undergoes a rapid and transient translocation to bacterial entry sites, an event promoted by SigD/SopB. Recruitment of SNX1 to SCVs results in the formation of extensive, long-range tubules that we have termed 'spacious vacuole-associated tubules'. Formation of these tubules is coupled with size reduction of vacuoles and the removal of TGN-resident cargo. SNX1 suppression perturbs intracellular progress of bacteria, resulting in a delayed replication. We propose that SNX1 is important in tubular-based re-modeling of nascent SCVs and, in doing so, regulates intracellular bacterial progression and replication.**

Supplementary material available online at
http://jcs.biologists.org/cgi/content/full/121/12/2027/DC1

Key words: Phosphoinositide, *Salmonella*, SCV, Endosome, Retromer, SigD, Sorting nexin

Introduction

Salmonella enterica serovar Typhimurium (*S. Typhimurium*) invade non-phagocytic cells by actively inducing their uptake and thereby enabling the pathogens to escape immune responses and to establish a replication niche within the host cell (Knodler and Steele-Mortimer, 2003). Following internalization, *S. Typhimurium* resides in a specialized membranous organelle, termed the *Salmonella*-containing vacuole (SCV). In many ways newly formed SCVs resemble early endosomes, being enriched in phosphatidylinositol 3-monophosphate [PtdIns(3)*P*] (Pattni et al., 2001) and recruiting many PtdIns(3)*P*-interacting proteins including EEA1 (Steele-Mortimer et al., 1999). One important *Salmonella* effector that is delivered into the host cell cytosol through the *Salmonella* type III secretion system (Yip and Strynadka, 2006; Gruenberg and van der Goot, 2006) is SigD, also known as SopB (Norris et al., 1998; Steele-Mortimer et al., 2000; Marcus et al., 2001; Terebiznik et al., 2002). SigD/SopB is an inositol polyphosphate phosphatase that has been proposed to dephosphorylate a wide range of host phosphoinositides and thereby allow early SCVs to gradually mature into 'late SCVs' (Gorvel and Meresse, 2001). Here they become acidified (Rathman et al., 1996; Drecktrah et al., 2007) and acquire late endosomal markers, such as Rab7, and lysosomal glycoproteins including Lamp1 (Meresse et al., 1999; Steele-Mortimer et al., 1999). Nevertheless, because of the reported absence of certain late endosomal markers, for example the CI-MPR (Garcia-del Portillo and Finlay, 1995), it has been argued that there is limited, or selective, interaction between SCVs and membranes of the late endosomal network. Further still, the marked delay in acquisition of cathepsin D and cathepsin L indicates that maturation kinetics of SCV biogenesis are slowed compared with endosomal maturation (Garcia-del Portillo and Finlay, 1995; Steele-Mortimer et al., 1999). However, the recent demonstration of an unexpected degree of interactions of SCVs with late endosomal and/or lysosomal markers has argued against such a selective interaction of SCVs with the endo-lysosomal system (Drecktrah et al., 2007).

The family of mammalian sorting nexins (SNXs) comprises over thirty members, many of which have been implicated in various aspects of endosomal biology (Worby and Dixon, 2002; Carlton et al., 2005). The unifying hallmark of this family is a sorting nexin phox (PX)-homology domain. In the case of the prototypical family member, sorting nexin-1 (SNX1), this PX domain binds to PtdIns(3)*P* and phosphatidylinositol (3,5)-bisphosphate [PtdIns(3,5)P_2] (Cozier et al., 2002). This aids the targeting of SNX1 to elements of the PtdIns(3)*P*-rich and PtdIns(3,5)P_2-rich endosomal network, where it partially colocalizes with markers of the early endosome, but not with late endosomal and/or lysosomal markers (Carlton et al., 2004). Besides the phosphoinositide-binding PX domain, SNX1 possesses an additional membrane-binding module, namely a BAR (Bin-amphiphysin-Rvs) domain. This domain conveys the ability to sense membrane curvature and induce membrane tubulation (Carlton et al., 2004; Peter et al., 2004; McMahon and Gallop, 2005). Thus, in vitro recombinant SNX1

induces, or stabilizes, tubulation of artificial liposomes in a concentration-dependent fashion, and in vivo, overexpression of SNX1 results in extensive tubulation of early endosomes (Carlton et al., 2004). Through the combined properties of its PX and BAR domains, SNX1 is targeted to phosphoinositide-enriched narrow-diameter membrane tubules emanating from the early endosome. From here, as part of the retromer complex, SNX1 facilitates transport of hydrolase receptors such as the cation-independent mannose 6-phosphate receptor (CI-MPR) back to the *trans*-Golgi network (TGN) (Arighi et al., 2004; Carlton et al., 2004; Seaman, 2004).

In light of the debate surrounding the issue of whether SCVs interact in a selective manner with the endo-lysosomal system (Drecktrah et al., 2007), one piece of evidence in favor of this model being the lack of detectable CI-MPR on the SCV (Garcia-del Portillo and Finlay, 1995), we have here explored the role of SNX1 in SCV biogenesis and bacterial replication. Using live-cell and immunofluorescence microscopy, combined with RNA interference (RNAi) and bacterial replication assays, we show that SNX1 is recruited to nascent SCVs inducing the dynamic tubular-based re-modeling of this compartment. Consistent with these tubules functioning in the retrograde transport of CI-MPR, RNAi-mediated suppression of SNX1 expression results in the appearance of CI-MPR on SCVs, an observation that argues against a selective interaction of SCVs with the endo-lysosomal system. Finally, we show that SNX1-induced re-modeling is important for SCV biogenesis because suppression of SNX1 leads to a defect in the intracellular progression and replication of invaded *Salmonella*.

Results

SNX1 is readily recruited to the site of *Salmonella* invasion

In uninfected cells, SNX1 localizes to early endosomes throughout the cell, with a slight enrichment in the perinuclear area (Fig. 1A). However, when infected with the *S. Typhimurium* strain SL1344, within 15 minutes post infection, the subcellular distribution of SNX1 was markedly altered. In these cells, SNX1 underwent redistribution to sites of bacterial cell entry and was found clustered underneath actin-rich membrane ruffles (Fig. 1B). Even 60 minutes post infection, SNX1 remained clustered around the invading bacteria, which at this time had further progressed toward the perinuclear area (Fig. 1C). At later time points (3 hours post infection, Fig. 1D), SNX1 was no longer found localized to bacteria, and displayed a distribution indistinguishable from the distribution observed prior to infection. Analysis of the kinetics of protein acquisition revealed that the redistribution of SNX1 to the SCV (see below) was rapid and transient (Fig. 1E), with the extent and kinetics in MDCK cells being comparable with those observed in HeLa cells (Fig. 1F).

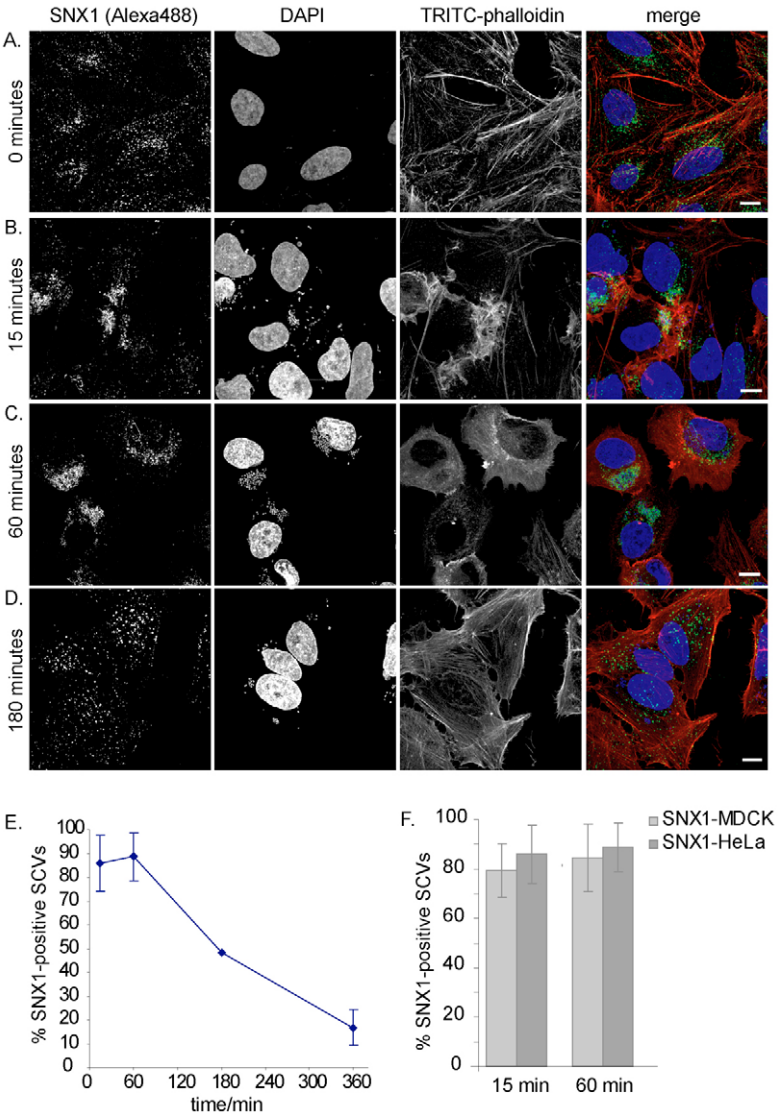

Fig. 1. SNX1 is recruited to sites of *Salmonella Typhimurium* entry. HeLa cells were either fixed directly, or were infected with SL1344 for 15 min and fixed at indicated times. Cells were immunolabeled using anti-SNX1 (Alexa488, green) and stained with TRITC-phalloidin to visualize actin (red) and DAPI to label DNA (blue). (A) In uninfected cells, SNX1 displayed a cytoplasmic distribution with perinuclear enrichment. (B) SNX1 was recruited to invasion sites, readily identifiable by membrane ruffles, and (C) stayed associated with the bacteria. (D) After 180 minutes, SNX1 had resumed its original distribution. (E) For the kinetic analysis of SNX1 association with SCVs, between 50–150 SCVs were scored per assay per time point for the presence or absence of SNX1 ($n \geq 6$ for 15 minutes and 60 minutes ± standard deviation, s.d.; $n=2$ for 180 minutes and 360 minutes, error ± minimum or maximum). (F) SNX1 recruitment to SCVs is comparable in MDCK ($n=4$, ± s.d., 50–150 SCVs scored per assay) and HeLa cells ($n>3$, ± s.d.), analyzed after a 15-minute bacterial 'pulse' or further 45 minutes incubation. Scale bar: 10 μm.

SNX1 is recruited to nascent and maturing SCVs

To analyze the distribution of SNX1 during infection in more detail, optical *z*-sections from cells after 15 minutes infection were deconvolved, and subsequently 3D-rendered and animated to allow a '360° view'. This analysis revealed that, at this time point, SNX1 had accumulated on SCVs in a non-uniform fashion (Fig. 2A top inset) at the base of actin-rich membrane ruffles (Fig. 2B,C; Movie 1). Interestingly, in some instances tubular-like profiles decorated with SNX1 were observed around the site of bacterial infection (Fig. 2C).

The observed globular or meshwork-like manifestation of SNX1 at the site of infection was furthermore markedly different from recruited EEA1 that exhibited a discrete vesicular pattern (Fig. 2D). Compared with EEA1, SNX1 also stayed associated with bacteria

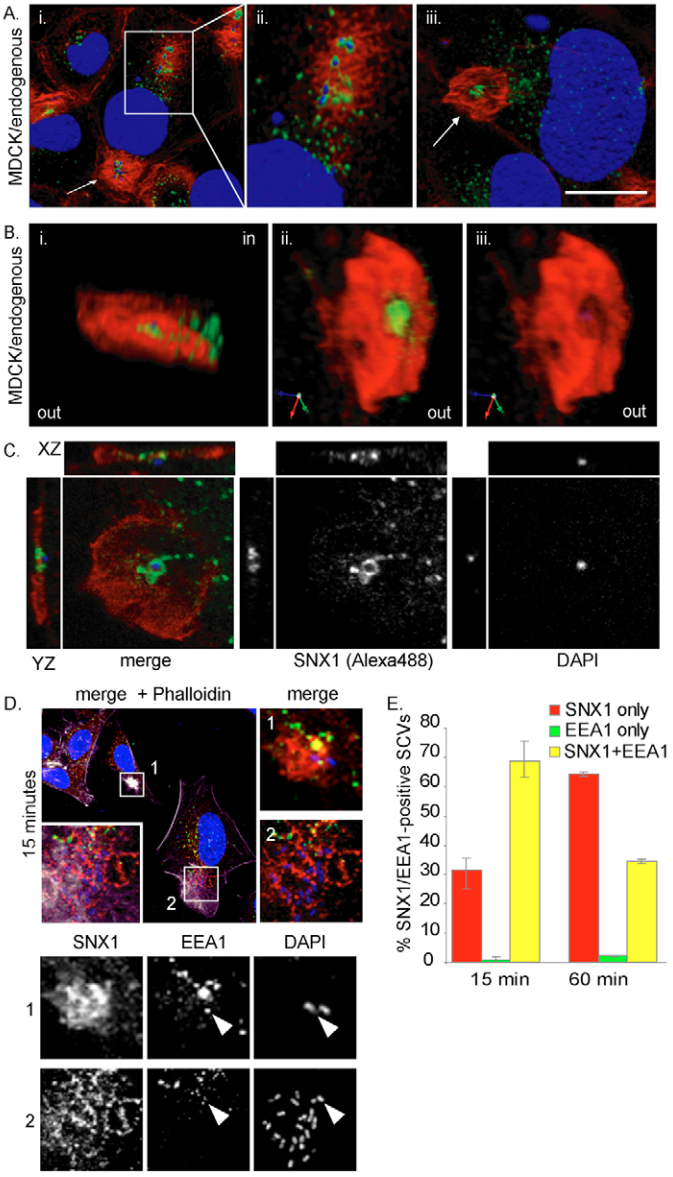

Fig. 2. Further analysis of SNX1-recruitment to plasma membrane ruffles and SCVs. (A-C) MDCK cells were infected with the SL1344 strain for 15 minutes, then fixed and immunolabeled. Ten optical *z*-slices were deconvolved and 3D-image volume rendered (see also supplementary material Movie 1). (Ai-iii) SNX1 (green) clearly accumulates at membrane ruffles (arrows) and around bacteria (boxed area in Ai, magnification in Aii). (B) Magnification of the membrane ruffle shown in (Aiii), with the green (SNX1) channel omitted in (Biii). (C) A single optical *z*-section of the maximum projections shown in (Aiii) and (B), respectively, is displayed with insets providing the respective *YZ*- and *XZ*-view. Note that SNX1 is localized as a ring around the bacterium. (D) HeLa cells infected with SL1344 for 15 minutes were fixed, immunolabeled for endogenous SNX1 (Alexa594, red) and EEA1 (Alexa488, green), and labeled with DAPI (blue) and TRITC-phalloidin (magenta). Whereas SNX1 appears as globular or tubular at sites of infection, EEA1 displays a punctate distribution (arrowheads). (E) Quantification of SNX1 and EEA1 acquisition on SCVs, scoring between 40-100 SCVs in individual *z*-sections, expressed as percentage of all SNX1- and/or EEA1-positive bacteria (n=3 for 15 minutes, n=2 for 60 minutes, error ± minimum or maximum). Scale bar: 10 μm.

for a prolonged period (Fig. 2E) consistent with SNX1 associating with both 'nascent' and 'maturing' SCVs.

Recruitment of GFP-SNX1 to SCVs triggers formation of spacious vacuole-associated tubules and coincides with vacuolar shrinking

The rapid and prolonged, yet transient recruitment of SNX1 to the site of invasion prompted us to investigate the dynamics of this process in more detail using live-cell imaging. MDCK cells were transiently transfected with a plasmid encoding GFP-SNX1. Confirming our fixed-cell analyses, GFP-SNX1 was readily recruited to the site of invasion within 15 minutes post infection, resulting in a loss of SNX1 from the perinuclear pool (Fig. 3A,B, supplementary material Movie 2a-d; similar data obtained for HeLa cells, but not shown). Strikingly, recruitment coincided with the appearance of numerous long-range GFP-SNX1-positive tubules, which emanated from the site of infection and appeared to be shooting off from the SCVs. In some cases, tubules were observed to make contact with vesicular pools of SNX1 (boxed area in Fig. 3A,B). As GFP-SNX1 recruitment was most pronounced at large vacuolar structures we termed these tubules 'spacious vacuole-associated tubules', or SVATs. Strikingly, tubulation was concomitant with rapid size-reduction of spacious vacuoles. To estimate the kinetics of this process, we analysed within the same visual field the shrinkage rate of large vacuoles in GFP-SNX1-expressing and infected cells versus non-transfected yet infected cells (Fig. 3C-E). Here, the difference in the area over time (in frames) of light-lucent spacious vacuoles was determined; in cells visibly forming SVATs, the vacuoles shrank approximately 2.5 times faster than in non-transfected cells. To better visualize the full extent of tubulation, cells expressing GFP-SNX1 and infected with SL1344 were fixed prior to confocal imaging across various z-sections. Subsequent deconvolution and 3D-rendering revealed an extensive tubular meshwork of GFP-SNX1 around the invading bacteria 15 minutes post infection (see Fig. 4A; Movie 3).

In previous imaging studies of endogenous SNX1 (see Figs 1 and 2), where cells were fixed at 4°C in 2% PFA, only some SNX1-decorated tubules were present, although these were not as extensive as observed with overexpressed SNX1. To therefore verify that tubules were not an artefact of SNX1 overexpression, we optimized fixation conditions to retain tubular morphology. By fixing infected cells at 37°C in DMEM supplemented with 4% PFA, tubules decorated with endogenous SNX1 of up to 25 μm in length were routinely observed in both HeLa and MDCK cells (Fig. 4B-C, Fig. 5B). Taken together, these data establish that, upon *Salmonella* infection, SNX1 is recruited to the site of infection, including the nascent SCV from where the formation of an extensive array of dynamic membrane tubules is induced.

SNX1 recruitment dynamics are altered when infecting with a *Salmonella* strain that lacks SigD

SigD, also known as SopB (Hong and Miller, 1998; Norris et al., 1998), is a bacterial phosphatidylinositol phosphatase that is injected into the host cell upon infection. Currently, the literature is divergent about the substrate specificity; amongst others PtdIns(4,5)P_2 (Terebiznik et al., 2002; Mason et al., 2007) and – from in vitro studies – PtdIns(3,5)P_2 and PtdIns(3,4,5)P_3 (Norris et al., 1998; Marcus et al., 2001) have also been proposed as substrates. Infection of Henle-407 cells with a *Salmonella* strain that lacks SigD (ΔsigD) results in the formation of only small vacuoles that, additionally, rarely fused with one another (Hernandez et al., 2004). Likewise, ectopic overexpression of SigD in mammalian cells has been shown

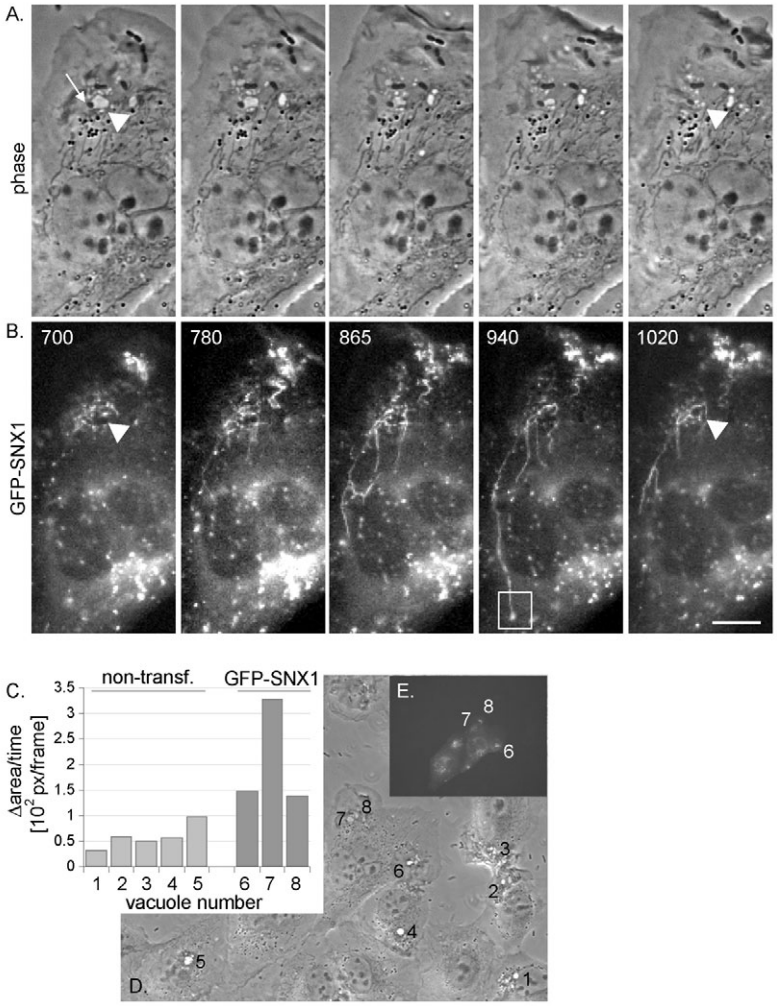

Fig. 3. SNX1 recruitment induces long-range tubules appearing concomitant with vacuolar shrinking. MDCK cells expressing GFP-SNX1 were infected with the SL1344 strain and invasion was imaged live (see supplementary material Movie 2a-d). Selected frames of a region of interest are shown (time in seconds). (A) Phase contrast images. Note the size reduction of vacuoles (arrowhead) at vacuole containing bacteria (arrow). (B) GFP-SNX1 was readily recruited to bacteria and spacious SCVs and labeled long-rage tubules; these spacious vacuole-associated tubules (SVATs) were also occasionally observed to make contact with vesicular SNX1 pools (boxed area). (C-E) Analysis of vacuolar shrinking. (C) The changes of vesicle area (in pixels) per frame of one focal depth from movies of LCI infection assays were analyzed from randomly chosen large light-lucent vesicles (see D) in infected cells expressing GFP-SNX1 (vesicles 6-8, compare E) or non-transfected yet infected cells (1-5). Data are representative for over n=3 independent experiments for each cell type (HeLa or MDCK cells) with over ten cells imaged.

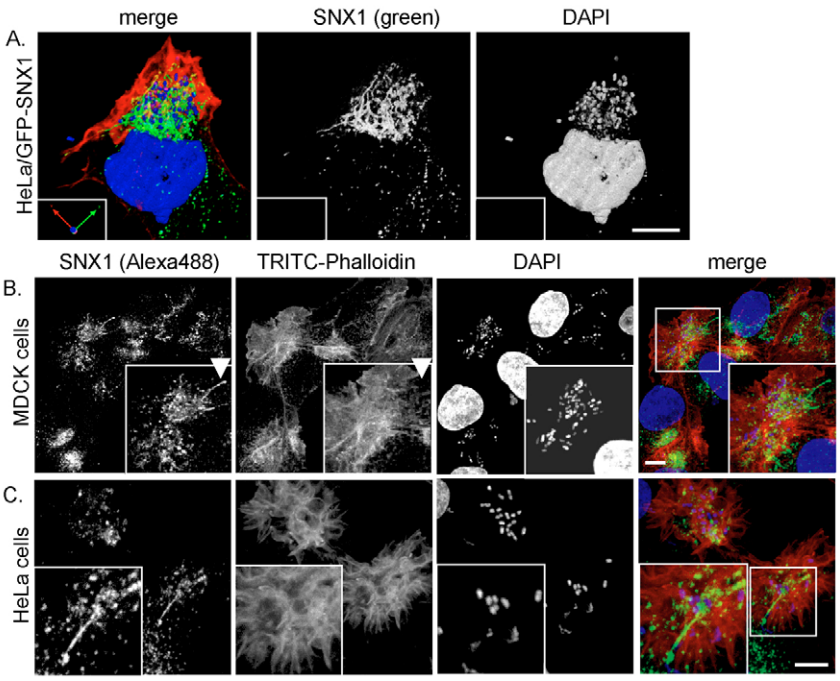

Fig. 4. Further characterization of SVATs. (A) HeLa cells expressing GFP-SNX1 were infected with SL1344, fixed after a 15-minute infection and treated with TRITC-phalloidin and DAPI. GFP-SNX1 (green) creates a meshwork around bacteria (blue). Images of a deconvolved stack are shown (see supplementary material Movie 3). (B,C) Tubulation is not an artifact of overexpressing GFP-SNX1. Cells infected for 15 minutes were fixed using 4% paraformaldehyde at 37°C for 15 minutes and immunolabeled for endogenous SNX1 (Alexa488, green). Scale bar: 10 μm.

to induce formation of large vacuoles (Terebiznik et al., 2002; Dukes et al., 2006; Mason et al., 2007).

When we analyzed recruitment of SNX1 in HeLa cells infected with a ΔsigD *Salmonella* strain, we failed to observe the generation of spacious vacuoles, as evidenced by the lack of large light-lucent structures in the phase-contrast images (Fig. 5A, supplementary material Movie 4b). Moreover, we did not observe significant accumulation of GFP-SNX1 at the site of infection (Fig. 5, arrowheads) although tubulation from intracellular compartments that were not in direct contact with bacteria was evident (Fig. 5, arrows). This was also the case when examining the localization of endogenous SNX1; again we observed a lack of recruitment and tubulation when using the ΔsigD *Salmonella* strain (Fig. 5B,C). Finally, the recruitment of SNX1 and the generation of SVATs were restored in control cells infected with a SL1344-ΔsigD mutant complemented with a plasmid encoding for SigD (supplementary material Fig. S1, Movie 5a,b). Such data demonstrate that the recruitment of SNX1 to the site of infection and nascent SCVs requires the bacterial effector SigD, which is entirely consistent with the previously characterized PtdIns(3)*P*-binding properties of the SNX1-PX domain (Cozier et al., 2002).

SNX1 suppression leads to CI-MPR accumulation at infection sites

The CI-MPR is a hydrolase receptor that continuously cycles between endosomes and the TGN, but is almost exclusively localized to the TGN at steady-state (Ghosh et al., 2003). The virtual absence of the CI-MPR on SCVs has been regarded as indicative for a selective interaction of SCVs with components of the late endosomes. Indeed, as reported previously (Garcia-del Portillo and Finlay, 1995), we failed to observe significant accumulation of CI-MPR on SCVs upon infection with *S. Typhimurium* in control cells (Fig. 6A). Although at first this appears to support that SCVs do not markedly interact with CI-MPR-containing endosomes, there is growing evidence that the CI-MPR undergoes retrieval from an endosomal compartment (Arighi et al., 2004; Seaman, 2004) through a pathway that requires SNX1 (Carlton et al., 2004). Indeed, when we infected SNX1-suppressed cells with *Salmonella* for 15 minutes, we found extensive localization of CI-MPR at the site of invasion and on nascent SCVs (Fig. 6A). Thus, during infection, *Salmonella* do interact with host cell membranes from compartments containing the CI-MPR. However, since SNX1 – as part of the retromer complex (Arighi et al., 2004; Carlton et al., 2004; Seaman, 2004) – efficiently drives tubular-based retrograde transport of this receptor, at steady-state the CI-MPR is not observed to be enriched at the site of infection or the forming SCV.

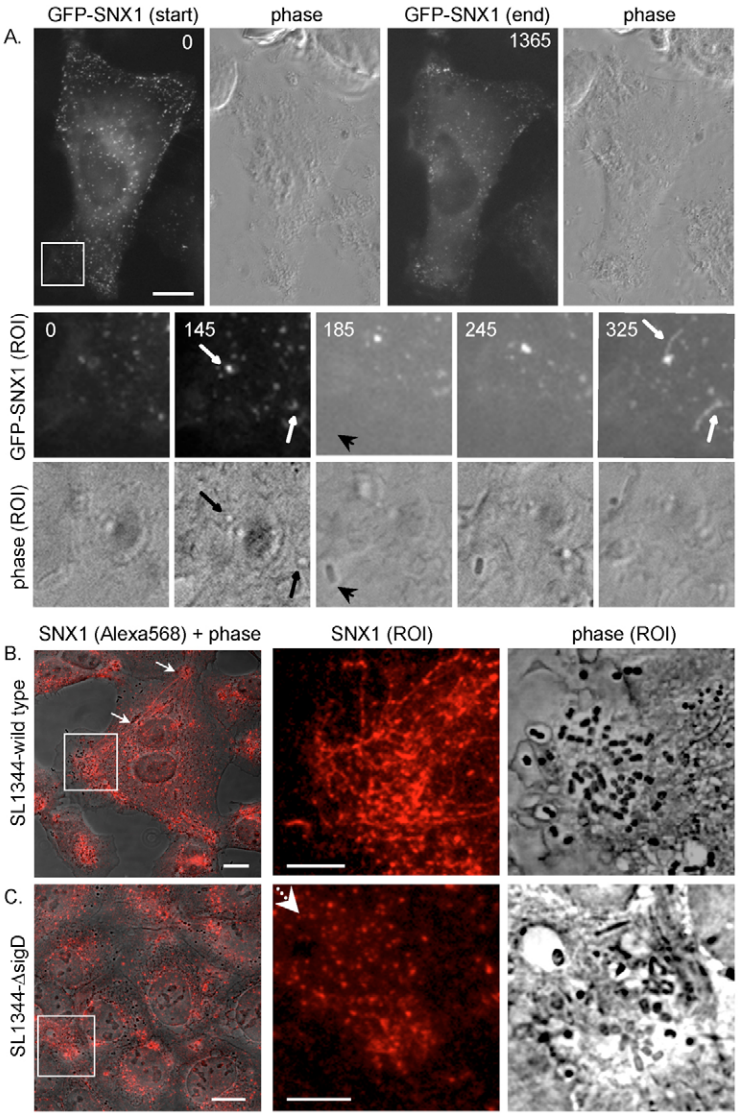

Fig. 5. No substantial recruitment of SNX1 was seen upon infection with a mutant strain that lacked SigD. (A) Cells expressing GFP-SNX1 were infected with a SL1344 strain lacking the inositol phosphatase SigD (ΔsigD) and infection was imaged for >20 minutes. Selected frames are shown (see also supplementary material Movie 4a,b). Although SNX1-positive tubules from endosomal structures were observed (arrows), there was no pronounced enrichment of GFP-SNX1 at the site of infection (arrowheads). (B) MDCK cells were infected a with wild-type SL1344 or with a SL1344-ΔsigD strain for 15 minutes, then fixed and labeled for endogenous SNX1 (Alexa568, red). Maximum projections of two *z*-sections (at 488 nm *z*-separation) are shown. Tubules up to 25 μm could be preserved in control cells (arrows). In SL1344-ΔsigD-infected cells, SNX1 is mainly vesicular with no pronounced recruitment to bacteria or even to very large vacuoles (arrowhead). Scale bar: 10 μm.

In SNX1-suppressed cells, intracellular progress of bacteria is markedly slowed

Besides an accumulation of the CI-MPR, it was apparent that in SNX1-suppressed cells, invading bacteria appeared less tightly clustered compared with control cells (Fig. 6B). Even 60 minutes post infection, a marked proportion of bacteria was still found in the cell periphery (Fig. 6C). To further characterize this 'scattering', we sought to quantify the difference in intracellular progress of bacteria under SNX1-suppressed conditions compared with controls. Therefore, we analyzed the distance that was covered by each individual bacterium from the plasma membrane to the nucleus after 180 minutes of infection for the different treatment conditions (Fig. 7). This revealed that, in control cells, the bacteria had covered on average 77.6% (median) of the distance to the nucleus (Fig. 7A), corresponding to a mean distance of 2.07 μm (± 1.2 μm s.d.) from the nucleus (Fig. 7C). By contrast, in SNX1-suppressed cells bacteria had covered a significantly shorter distance in the same time, being 4.03 μm (± 2.2 μm, s.d.) away from the nucleus (Fig.

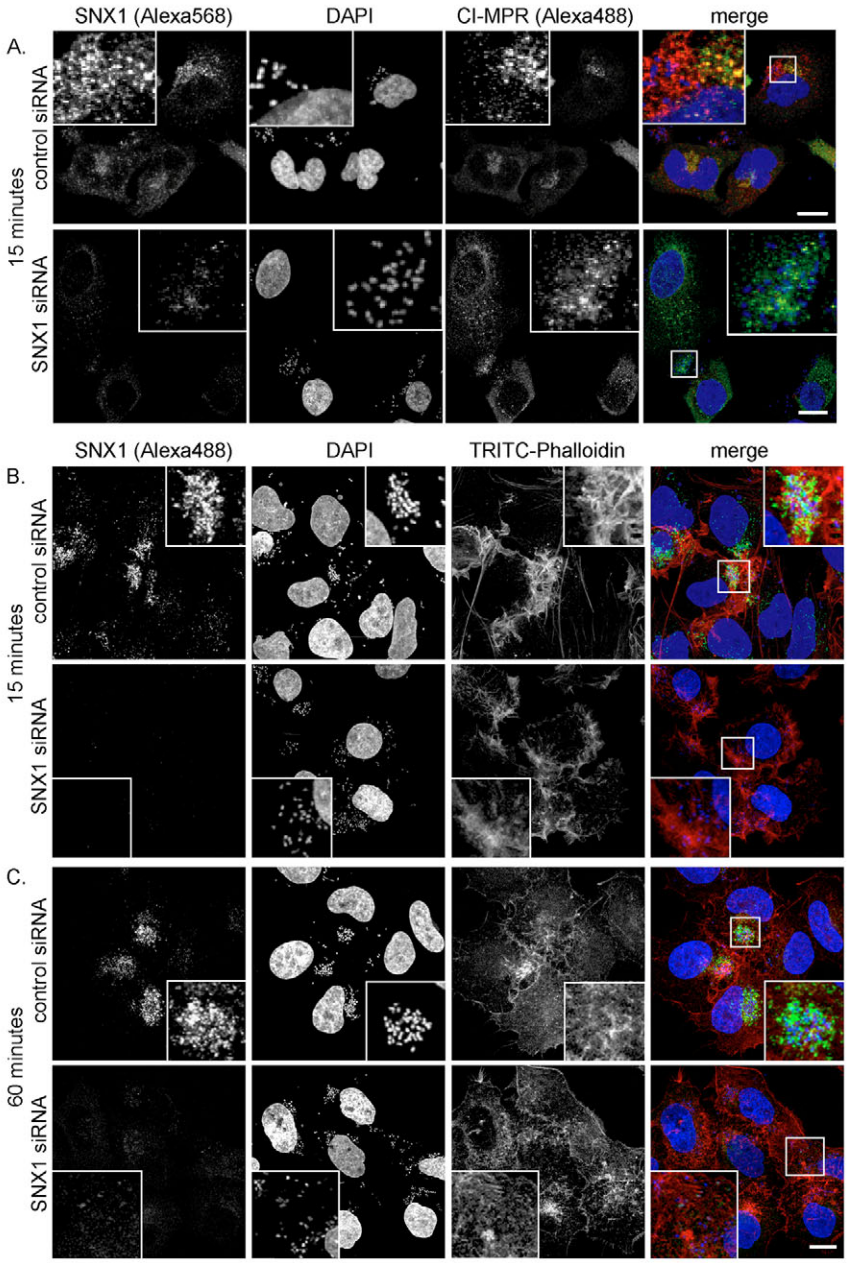

Fig. 6. Characterization of infection of SNX1-suppressed cells. Control and SNX1-suppressed cells were infected with SL1344 for 15 minutes, fixed and immunolabeled with anti-SNX1 and treated with DAPI. (A) Additionally, cells were immunolabeled with anti-CI-MPR (Alexa488, green). In SNX1-suppressed cells, the CI-MPR is redistributed to the site of bacterial entry. (B) After removing bacteria, cells were either fixed directly or after further 45 minutes, and additionally labeled with TRITC-phalloidin (red). In SNX1-suppressed cells, *S. Typhimurium* displays reduced clustering. Scale bar: 10 μm.

7C). Almost a third of the bacteria in SNX1-suppressed cells had covered less than 50% of the distance to the nucleus (Fig. 7B) compared with only 10% in the control cells (Fig. 7A). So, in SNX1-suppressed cells, a large fraction of bacteria appeared stalled in close proximity to the plasma membrane. Such data is consistent with a role for SNX1 in the progression of invading *Salmonella* inside the host cell.

In SNX1-suppressed cells, the onset of *Salmonella* replication is delayed

In phagocytes, the maintenance of spacious phagosomes has been suggested to contribute to bacterial virulence and survival (Alpuche-Aranda et al., 1994). However, our data has established that in epithelial cells SNX1 reduces the size of macropinosomes and SCVs. We thus sought to determine the effect of SNX1 on *Salmonella* virulence in epithelial cells in more detail by examining the effect of SNX1 suppression on bacterial invasion and replication. Therefore, we combined RNAi and population-based colony-forming unit (CFU) assays. These analyses showed that at early time points the averaged number of intracellular bacteria in SNX1-suppressed cells was comparable with those observed in control cells (Fig. 8, 1 hour time point). By contrast, at 6 hours post infection an approximately ninefold increase in the average number of intracellular bacteria was observed in control cells, whereas replication in SNX1 suppressed was only increased twofold. These findings are indicative of a delay in onset of replication in SNX1-suppressed cells and establish the importance of endogenous SNX1 for efficient *Salmonella* replication.

Discussion

It is well established that *Salmonella Typhimurium* can influence the endosomal system of host cells in very sophisticated ways to

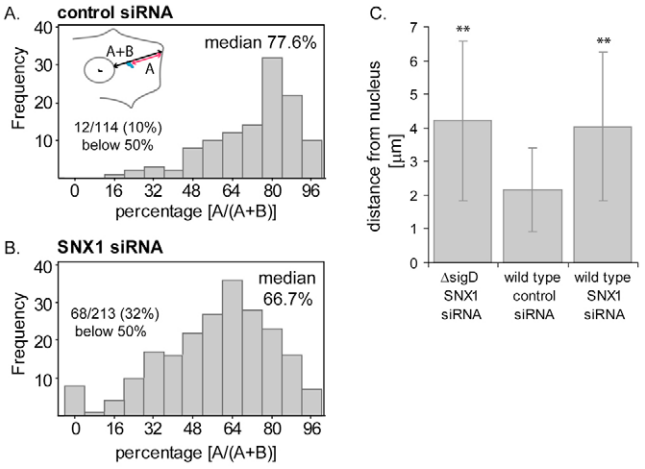

Fig. 7. In SNX1-suppressed cells, bacterial progress is slowed. (A,B) Analysis of intracellular progress of wild-type and ΔsigD bacteria in control and SNX1-suppressed cells. After 15 minutes, non-internalised bacteria were removed from siRNA-treated cells. Cells were subsequently fixed after a total of 180 minutes of incubation. After appropriate immunolabeling, cells were imaged and the distance covered by bacteria from the plasma membrane to the nucleus was measured for individual bacteria and expressed as a percentage of distance covered (at least 100-200 bacteria were measured). (C) Graphical representation of distance of bacteria from nucleus for wild-type and ΔsigD bacteria in control or SNX1 suppressed cells (± s.d). All *P*-values were calculated as comparisons with the wild-type value using a one-way ANOVA, followed by a post-hoc test (see Materials and Methods); $^{**}P<0.01$.

generate a unique vacuolar compartment in which it resides and eventually replicates. The still growing list of endosomal proteins targeted to these vacuoles shows how seamlessly the SCVs 'blend in' with the endosomal system and how effectively the pathogen has adapted to its host. Although the functional significance of host cell-components for SCV biogenesis is in many cases still unclear, we present evidence here that SNX1 is crucially involved in remodeling early stages of nascent SCVs.

We have established that, within 15 minutes of *Salmonella* infection, SNX1 undergoes a rapidly shift from its typically dispersed early endosomal location to one that is enriched on membranes that lie immediately below the site of bacterial entry. The enrichment of SNX1 occurs on large vacuoles, including nascent SCVs, and requires the *Salmonella* effector SigD. As SigD

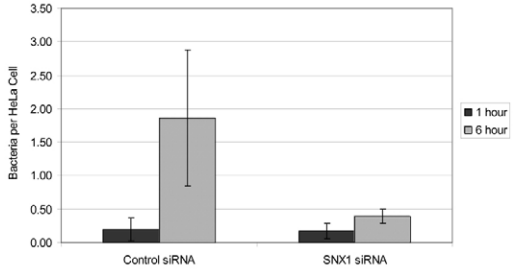

Fig. 8. In SNX1-suppressed cells, bacterial onset of replication is delayed. Analysis of bacterial replication kinetics in control and SNX1-suppressed cells for SL1344. The averaged number of bacteria per HeLa cell were determined at indicated times. Data are from a representative experiment with replicative efficiency being determined in triplicate (error bars shown ±s.d.). Similar data were observed in two additional independent assays.

is known to contribute to the large increase in PtdIns(3)*P* observed upon these vacuoles following *Salmonella* infection (Hernandez et al., 2004), the enrichment of SNX1 to these structures appears to be driven, in part, through the ability of its PX domain to bind this phosphoinositide. Compared with other PtdIns(3)*P*-binding proteins such as EEA1, however, the enrichment of SNX1 is more prolonged. This is unlikely to be a result from their respective affinities for this phosphoinositide, because the K_d for PtdIns(3)*P* of the SNX1-PX domain (micromolar range) is considerably higher than the K_d of EEA1 (nanomolar range) (Gaullier et al., 2000; Cozier et al., 2002; Zhong et al., 2002). However, the difference might reflect the more promiscuous binding profile of the SNX1-PX domain – because it can also bind PtdIns(3,5)P_2 with a comparable micromolar affinity (Cozier et al., 2002) – and the presence of an additional membrane-binding BAR domain. Interestingly, the enzyme that generates PtdIns(3,5)P_2 through phosphorylation of PtdIns(3)*P*, the early endosome-associated kinase PIKfyve (also known as PIP5K3) (Rutherford et al., 2006; Michell et al., 2006), is recruited to macropinosomes and SCVs during *Salmonella* infection (our unpublished data). PtdIns(3,5)P_2 might therefore be generated upon these structures, aiding and prolonging the enrichment of SNX1 compared with 'pure' PtdIns(3)*P*-binding proteins.

Once enriched on macropinosomes and SCVs, SNX1 localizes to an extensive network of membrane tubules that is highly dynamic and can, in some instances extend from one side of the cell to the other. These tubules are observed within 15 minutes of *Salmonella* infection and, therefore, they appear distinct to the previously characterized *Salmonella*-induced filaments (Sifs), which typically form 4-6 hours after invasion (Garcia-del Portillo et al., 1993; Stein et al., 1996). We have named these previously undescribed SNX1-labeled tubules 'spacious vacuole-associated tubules' (SVATs). Whether SNX1 actually drives the formation of SVATs or whether it is simply recruited to these tubules through its abilities to bind PtdIns(3)*P* and/or PtdIns(3,5)P_2-containing membranes of high curvature (Carlton et al., 2004) remains unclear. However, we have previously shown through in vitro and in vivo assays that in a concentration-dependent manner, SNX1 can drive the formation of membrane tubules (Carlton et al., 2004). We propose a model in which the enrichment and hence increase in local concentration of SNX1 on the spacious vacuoles actually drives the formation of SVATs. The concentration-dependency of this process might well arise from the ability of BAR domains to form dimers that, by forming a higher ordered lattice network, drives and stabilizes the formation of membrane tubules (Shimada et al., 2007; Frost et al., 2008).

Analyzing the kinetics of SVAT formation has revealed that they coincide with the shrinking of the spacious vacuoles – a phenomenon that would appear to arise from the increase in membrane exit elicited by the formation of SVATs. In macrophages, it has long been known that phagosomes gradually contract en route to the perinuclear area (Racoosin and Swanson, 1993). During *S. Typhimurium* infection however, the maintenance of spacious vacuoles appears to have an important role for optimal virulence in macrophages (Alpuche-Aranda et al., 1994). Accordingly, bacterial mutants that are defective in generating or maintaining large SCVs are attenuated in replication and survival (Alpuche-Aranda et al., 1994; Hernandez et al., 2004). Our data from the replication efficiency of *Salmonella* in SNX1-suppressed epithelial cells suggests that size reduction is necessary for optimal replication. This correlates with a decrease in the rate at which bacteria progress from the site of entry to their position

close to the TGN, where replication occurs (Beuzon et al., 2000; Salcedo and Holden, 2003; Abrahams et al., 2006; Deiwick et al., 2006). These data are thus consistent with a model in which the SNX1-dependent formation of SVATs has the effect of removing membrane, thereby decreasing the size of spacious vacuoles (including SCVs), hence aiding their movement through the host cell towards their site of replication.

That membrane is being removed from the SCVs through the SVATs is evident from the trafficking of the CI-MPR. At steady-state, this transmembrane receptor is almost exclusively localized to the TGN although it is undergoing continuous transport between this compartment and the plasma membrane and endocytic network (Waguri et al., 2003; Lin et al., 2004). In cells depleted of SNX1, retrograde transport of the CI-MPR from the endosomal network back to the TGN is perturbed such that the receptor shifts its steady-state and becomes enriched within endosomes (Carlton et al., 2004). Thus, upon infection of SNX1-suppressed cells with *Salmonella*, these 'pre-loaded' CI-MPR-containing endosomes are recruited to the site of infection, and the receptor becomes associated with SCVs. Such data demonstrate that membrane from CI-MPR-containing endosomes is recruited to the nascent SCV, but that SNX1 normally sorts this receptor for efficient removal through SVATs. These findings therefore explain the apparent anomaly that hydrolases delivered by the CI-MPR are found in SCVs; although, at steady-state, the receptor itself is not found on these vacuoles. In addition, these data support the emerging view that the biogenesis of SCVs do not occur through a previously envisaged selective interaction with elements of the endo-lysosomal system (see also Drecktrah et al., 2007).

Our data have clearly implicated a role for SNX1 in regulating the biogenesis of macropinosomes and SCVs formed upon *Salmonella* invasion. This raises the issue of whether other sorting nexins, in particular those SNXs that contain BAR domains, are also required for the biogenesis of these structures. Recently, sorting nexin-5 (SNX5) has been shown to undergo recruitment to macropinosomes formed after stimulation with epidermal growth factor (EGF) (Merino-Trigo et al., 2004; Kerr et al., 2006). Once recruited, SNX5 was observed on membrane tubules, the formation of which was dependent on the presence of SNX1 (Kerr et al., 2006). With evidence that SNX1 and SNX5 physically associate (Kerr et al., 2006; Wassmer et al., 2007), these data suggest that SNX1 is not the only sorting nexin that is recruited to and involved in the biogenesis of SCVs. Further work will be required to fully elucidate the role of these sorting nexins during *Salmonella* infection. Finally, sorting nexin-9 has recently been identified as one of the targets of the enteropathogenic *Escherichia coli* (EPEC) type III effector protein EspF (Marchès et al., 2006), an interaction that is used to promote EPEC pathogenesis and gastrointestinal disease (Alto et al., 2007). By defining the role of SNX1 in *Salmonella* infection our study further emphasizes the possibility that the mammalian sorting nexin family constitutes important cellular components whose functions are manipulated during host-pathogen interactions.

Materials and Methods

Antibodies and reagents

Monoclonal anti-SNX1 and anti-EEA1 antibodies were purchased from BD Biosciences. The polyclonal rabbit anti-SNX1 (human) antibody was a kind gift from Matthew Seaman (CIMR, Cambridge, UK) and was used successfully to immunolabel canine SNX1 in MDCK cells. The polyclonal rabbit anti-CI-MPR antibody was a kind gift from Paul Luzio (CIMR, Cambridge, UK). Monoclonal anti-Lamp-1 (H4A3) was from Research Diagnostics, Inc. The DAPI reagent and TRITC-labeled phalloidin were obtained from Sigma. The Rhodamine-TRITC-conjugated rabbit anti-goat IgG was purchased from Jackson ImmunoResearch Laboratories; all other secondary antibodies were obtained from Molecular Probes (Invitrogen). The goat anti-*Salmonella* CSA-1 antibody was from Kirkegaard and Perry Laboratories. If not stated otherwise, reagents were obtained from SigmaAldrich or Invitrogen.

DNA constructs

The original pEGFPC1-SNX1 construct was a kind gift from Rohan Teasdale (University of Queensland, Australia). Additionally for this study, using the *Age*I and *Bsr*GI restriction sites, the GFP-encoding sequence in the SNX1 vector was replaced with an mRFP-encoding sequence from the pmRFP vector, a kind gift from Roger Tsien (UCSD, CA), yielding an RFP-expressing chimeras of SNX1 (RFP-SNX1).

Transient transfections

HeLa (CCL-2) and MDCK cells, cultured as recommended by the ATCC (http://www.lgcpromochem.com/atcc), were plated on coverslips and transfected with vector DNA at 60% confluency using Genejuice (Novagen) according to the manufacturer's instructions. After 22 hours of incubation at 37°C in 5% CO_2, low-level expressing cells were used for respective experiments.

RNA interference

The previously characterized siRNA duplexes (Carlton et al., 2004) were purchased from Dharmacon (control target: 5′-AAGACAAGAACCAGAACGCCA-3′; SNX1 target: 5′-AAGAACAAGACCAAGAGCCAC-3′). HeLa cells were seeded at a density of 0.95×10^5 cells per 35-mm well. On the following day, cells were transfected with 100 nM siRNA duplex using Oligofectamine (Invitrogen) according to the manufacturer's instructions. After 60 hours, cells were trypsinized and for every transfection condition, several wells containing 120,000 cells per 16-mm well were seeded to ensure equal cell numbers. After further 12 hours, cells were used for experiments, and a subset of cells was harvested and lysed to assess the levels of SNX1 protein suppression by western blotting.

Bacterial strains

The wild-type strain SL1344, an isogenic SL1344-sigD deletion mutant (ΔsigD) and a SL1344-SigD strain complemented with a plasmid encoding SigD and its chaperone SigE (SL1344-sigD-pSigDE) were used (generously provided by Olivia Steele-Mortimer, NIAID, NIH, Hamilton, MT).

Bacterial infections

For all experiments, 100 μl of an overnight culture were diluted in 10 ml LB broth and grown to mid-log-phase while shaking for 3.5 hours at 37°C. For live-cell imaging and colony-forming unit assays, a multiplicity of infection (m.o.i.) of 50 in 1 ml of pre-warmed modified Krebs buffer (KB; 137 mM NaCl, 5.4 mM KCl, 1 mM $MgSO_4$, 0.3 mM KH_2PO_4, 0.3 mM NaH_2PO_4, 2.4 mM $CaCl_2$, 10 mM glucose and 10 mM Tris, adjusted to pH 7.4 at 37°C with HCl), was used.

Indirect immunofluorescence analysis

Fixed cells were permeabilized and immunolabeled with the respective primary and secondary antibodies and mounted on microscope slides using either Mowiol or Vectashield containing DAPI (Vector Laboratories) and analyzed by confocal microscopy.

Immunofluorescence imaging and data manipulation

Indirect immunofluorescence was performed using an Ultra^{VIEW} LCI Confocal Optical Scanner (PerkinElmer) or a Leica TCS-SP2-AOBS confocal laser-scanning microscope attached to a Leica DM IRE2 inverted epifluorescence microscope. Lenses used were 40× (HCX Apo) with 1.25 numerical aperture (NA) or 63× (PL ApoBL) with 1.4 NA oil-immersion objectives. Images were merged using Ultra^{VIEW} or Leica confocal software. Vol*ocity* software V4.0.1 (Impro*vision*) was used for compiling and compressing movies, deconvolution of data sets and 3D-image volume rendering. Where applicable, contrast and brightness adjustments for entire images only were made using Adobe Photoshop® 6.0 (Adobe Systems Inc.).

Infections for fixed-cell imaging

Cells washed twice with pre-warmed modified Krebs buffer (KB) were infected for 15 minutes in KB at 37°C. Bacteria were removed and cells were washed extensively with PBS, supplemented with 0.9 mM $CaCl_2$ and 0.5 mM $MgCl_2$ (PBS++). Cells were incubated in PBS++ for a further 15 minutes before being transferred into PBS++ supplemented with 16 μg/ml gentamicin to prevent further infection and being fixed using 2% PFA for 45 minutes at 4°C or 4% PFA for 15 minutes at 37°C to improve tubule preservation. All time points are given from the start of experiment, thus before infection.

Live-cell imaging

Transfected cells were washed twice with KB and coverslips were transferred to 1 ml imaging buffer (125 mM NaCl, 42 mM Hepes, pH 7.4, 18 mM glucose, 5.4 mM KCl, 3 mM $NaHCO_3$, 1.6 mM $MgCl_2$ and 1.3 mM EGTA). For image capturing, a

wide-field system (inverted Leica DMIRB microscope equipped with a Hamamatsu C4742-95 cooled CCD camera) combined with Openlab 4 software (Improvision) for automation was used. Three focal depths (1.5 µm apart) were captured at 20-second intervals; bacteria were added at the indicated m.o.i. and cells were imaged for 25-30 minutes.

Colony-forming unit assays

Cells treated with siRNA were washed twice with KB and infected with bacteria for 15 minutes (m.o.i. of 40-50), a protocol shown in preliminary optimization experiments to consistently result in the invasion of low numbers of *Salmonella* per cell. Bacteria were removed and cells were washed three times with PBS++, then incubated in modified KB for a further 15 minutes prior to transfer to DMEM containing 50 µg/ml gentamicin for 30 minutes. Cells were subsequently washed into DMEM that contained 10% FCS and 16 µg/ml gentamicin. At indicated times, cells were washed once with PBS++ and lysed (1% Triton X-100, 0.1% SDS in PBS), and a serial dilution of lysates in PBS++ was plated in replicates onto LB-agar plates. After incubation for 16 hours at 37°C, the number of colonies was determined.

Analysis of vacuolar shrinking in GFP-SNX1-expressing cells

Movies of real-time infection assays using MDCK cells transiently transfected with a vector encoding for GFP-SNX1 and infected with SL1344 bacteria were used. Using single frames of one focal depth (phase contrast, 1322×1024 pixels), shrinkage of vesicles was analyzed as difference in area over frames. It was chosen to analyze the largest, rounded vesicles (indicative for sealing) that also had visibly ceased interacting with other SCVs. The frame where the area of the vesicle in question was observed to be largest (determined using ImageJ, NIH Image) was deemed t(start); the end point was determined either by virtual disappearance of the vacuole or, when the end of the image sequence was reached, the area was measured again at this time point. Speed of shrinkage was determined as the difference in area ΔA(end-start), expressed in pixels over time (expressed in frames). These units were chosen to mirror the somewhat qualitative character.

Distance analysis

Maximum *z*-stack projections of images from bacterial infection and immunolabeling experiments of control and SNX1-suppressed cells were evaluated. In these cells, the distance covered from the plasma membrane and to the nucleus by each individual bacterium was determined. Distance covered of at least 100-200 bacteria per condition was analyzed.

Statistical analysis

Data from the distance analyses were analysed by a one-way ANOVA followed by Dunnett's multiple comparison post-hoc test using IGOR Pro 5.04B software package (WaveMetrics). The ANOVA indicated differences between the groups with $P<0.0001$ in the experiments. The values for the Dunnett's post hoc analysis were significant at $P<0.01$.

We thank Alan Leard and Emily de Looze for assistance with live-cell imaging. We thank the Medical Research Council for funding the School of Medical Sciences Cell Imaging Facility. M.V.B. is supported by the Department of Biochemistry, University of Bristol and PerkinElmer Life and Analytical Sciences. S.H. is supported by BBSRC and Unilever. Work in the laboratory of P.J.C. is supported by the Wellcome Trust.

References

Abrahams, G. L., Muller, P. and Hensel, M. (2006). Functional dissection of sseF, a type III effector protein involved in positioning the Salmonella-containing vacuole. *Traffic* **7**, 950-965.

Alpuche-Aranda, C. M., Racoosin, E. L., Swanson, J. A. and Miller, S. I. (1994). Salmonella stimulate macrophage macropinocytosis and persist within spacious phagosomes. *J. Exp. Med*. **179**, 601-608.

Alto, N. M., Weflen, A. W., Rardin, M. J., Yarar, D., Lazar, C. S., Tonikian, R., Koller, A., Taylor, S. S., Boone, C., Sidhu, S. S. et al. (2007). The type III effector EspF coordinates membrane trafficking by the spatiotemporal activation of two eukaryotic signaling pathways. *J. Cell Biol.* **178**, 1265-1278.

Arighi, C. N., Hartnell, L. M., Aguilar, R. C., Haft, C. R. and Bonifacino, J. S. (2004). Role of the mammalian retromer in sorting of the cation-independent mannose 6-phosphate receptor. *J. Cell Biol*. **165**, 123-133.

Beuzon, C. R., Meresse, S., Unsworth, K. E., Ruiz-Albert, J., Garvis, S., Waterman, S. R., Ryder, T. A., Boucrot, E. and Holden, D. W. (2000). Salmonella maintains the integrity of its intracellular vacuole through the action of SifA. *EMBO J*. **19**, 3235-3249.

Carlton, J., Bujny, M., Peter, B. J., Oorschot, V. M. J., Rutherford, A., Mellor, H., Klumperman, J., McMahon, H. T. and Cullen, P. J. (2004). Sorting nexin-1 mediates tubular endosome-to-TGN transport through coincidence sensing of high-curvature membranes and 3-phosphoinositides. *Curr. Biol*. **14**, 1791-1800.

Carlton, J., Bujny, M., Rutherford, A. and Cullen, P. (2005). Sorting nexins-Unifying trends and new perspectives. *Traffic* **6**, 75-82.

Cozier, G. E., Carlton, J., McGregor, A. H., Gleeson, P. A., Teasdale, R. D., Mellor, H. and Cullen, P. J. (2002). The phox homology (PX) domain-dependent, 3-phosphoinositide-mediated association of sorting nexin-1 with an early sorting endosomal compartment is required for its ability to regulate epidermal growth factor receptor degradation. *J. Biol. Chem*. **277**, 48730-48736.

Deiwick, J., Salcedo, S. P., Boucrot, E., Gilliland, S. M., Henry, T., Petermann, N., Waterman, S. R., Gorvel, J.-P., Holden, D. W. and Meresse, S. (2006). The translocated Salmonella effector proteins SseF and SseG interact and are required to establish an intracellular replication niche. *Infect. Immun*. **74**, 6965-6972.

Drecktrah, D., Knodler, L. A., Howe, D. and Steele-Mortimer, O. (2007). Salmonella trafficking is defined by continuous dynamic interactions with the endolysosomal system. *Traffic* **8**, 212-225.

Dukes, J. D., Lee, H., Hagen, R., Reaves, B. J., Layton, A. N., Galyov, E. E. and Whitley, P. (2006). The secreted Salmonella dublin phosphoinositide phosphatase, SopB, localizes to PtdIns(3)P-containing endosomes and perturbs normal endosome to lysosome trafficking. *Biochem. J*. **395**, 239-247.

Frost, A., Perera, R., Roux, A., Spasov, K., Destaing, O., Egelman, E. H., De Camilli, P. and Unger, V. M. (2008). Structural basis of membrane invagination by F-BAR domains. *Cell* **132**, 807-817.

Garcia-del Portillo, F. and Finlay, B. B. (1995). Targeting of Salmonella Typhimurium to vesicles containing lysosomal membrane glycoproteins bypasses compartments with mannose 6-phosphate receptors. *J. Cell Biol*. **129**, 81-97.

Garcia-del Portillo, F., Zwick, M. B., Leung, K. Y. and Finlay, B. B. (1993). Salmonella induces the formation of filamentous structures containing lysosomal membrane glycoproteins in epithelial cells. *Proc. Natl. Acad. Sci. USA* **90**, 10544-10548.

Gaullier, J.-M., Ronning, E., Gillooly, D. J. and Stenmark, H. (2000). Interaction of the EEA1 FYVE finger with phosphatidylinositol 3-phosphate and early endosomes. Role of conserved residues. *J. Biol. Chem.* **275**, 24595-24600.

Ghosh, P., Dahms, N. M. and Kornfeld, S. (2003). Mannose 6-phosphate receptors: new twists in the tale. *Nat. Rev. Mol. Cell Biol*. **4**, 202-212.

Gorvel, J. P. and Meresse, S. (2001). Maturation steps of the Salmonella-containing vacuole. *Microbes Infect.* **3**, 1299-1303.

Gruenberg, J. and van der Goot, F. G. (2006). Mechanisms of pathogen entry through the endosomal compartments. *Nat. Rev. Mol. Cell Biol*. **7**, 495-504.

Hernandez, L. D., Heuffer, K., Wenk, M. R. and Galan, J. E. (2004). Salmonella modulates vesicular traffic by altering phosphoinositide metabolism. *Science* **304**, 1805-1807.

Hong, K. H. and Miller, V. L. (1998). Identification of a novel Salmonella invasion locus homologous to Shigella ipgDE. *J. Bacteriol*. **180**, 1793-1802.

Kerr, M. C., Lindsay, M. R., Luetterforst, R., Hamilton, N., Simpson, F., Parton, R. G., Gleeson, P. A. and Teasdale, R. D. (2006). Visualisation of macropinosome maturation by the recruitment of sorting nexins. *J. Cell Sci.* **119**, 3967-3980.

Knodler, L. A. and Steele-Mortimer, O. (2003). Taking possession: biogenesis of the Salmonella-containing vacuole. *Traffic* **4**, 587-599.

Lin, S. X., Mallet, W. G., Huang, A. Y. and Maxfield, F. R. (2004). Endocytosed cation-independent mannose 6-phosphate receptor traffics via the endocytic recycling compartment en route to the trans-Golgi network and a subpopulation of late endosomes. *Mol. Biol. Cell* **15**, 721-733.

Marchès, O., Batchelor, M., Shaw, R. K., Patel, A., Cummings, N., Nagai, T., Sasakawa, C., Carlsson, S. R., Lundmark, R., Cougoule, C. et al. (2006). EspF of enteropathogenic Escherichia coli binds sorting nexin 9. *J. Bacteriol.* **188**, 3110-3115.

Marcus, S. L., Wenk, M. R., Steele-Mortimer, O. and Finlay, B. B. (2001). A synaptojanin-homologous region of Salmonella Typhimurium SigD is essential for inositol phosphatase activity and Akt activation. *FEBS Lett*. **494**, 201-207.

Mason, D., Mallo, G. V., Terebiznik, M. R., Payrastre, B., Finlay, B. B., Brumell, J. H., Rameh, L. and Grinstein, S. (2007). Alteration of epithelial structure and function associated with PtdIns(4,5)P_2 degradation by a bacterial phosphatase. *J. Gen. Physiol*. **129**, 267-283.

McMahon, H. T. and Gallop, J. L. (2005). Membrane curvature and mechanisms of dynamic cell membrane remodelling. *Nature* **438**, 590-596.

Meresse, S., Steele-Mortimer, O., Finlay, B. B. and Gorvel, J. P. (1999). The rab7 GTPase controls the maturation of Salmonella Typhimurium-containing vacuoles in HeLa cells. *EMBO J.* **18**, 4394-4403.

Merino-Trigo, A., Kerr, M. C., Houghton, F., Lindberg, A., Mitchell, C., Teasdale, R. D. and Gleeson, P. A. (2004). Sorting nexin 5 is localized to a subdomain of the early endosomes and is recruited to the plasma membrane following EGF stimulation. *J. Cell Sci.* **117**, 6413-6424.

Michell, R. H., Heath, V. L., Lemmon, M. A. and Dove, S. K. (2006). Phosphatidylinositol 3,5-bisphosphate: metabolism and cellular functions. *Trends Biochem. Sci*. **31**, 52-63.

Norris, F. A., Wilson, M. P., Wallis, T. S., Galyov, E. E. and Majerus, P. W. (1998). SopB, a protein required for virulence of Salmonella dublin, is an inositol phosphate phosphatase. *Proc. Natl. Acad. Sci. USA* **95**, 14057-14059.

Pattni, K., Jepson, M., Stenmark, H. and Banting, G. (2001). A PtdIns(3)P-specific probe cycles on and off host cell membranes during Salmonella invasion of mammalian cells. *Curr. Biol*. **11**, 1636-1642.

Peter, B. J., Kent, H. M., Mills, I. G., Vallis, Y., Butler, P. J., Evans, P. R. and McMahon, H. T. (2004). BAR domains as sensors of membrane curvature: the amphiphysin BAR structure. *Science* **303**, 495-499.

Racoosin, E. L. and Swanson, J. A. (1993). Macropinosome maturation and fusion with tubular lysosomes in macrophages. *J. Cell Biol*. **121**, 1011-1020.

Rathman, M., Sjaastad, M. and Falkow, S. (1996). Acidification of phagosomes containing Salmonella Typhimurium in murine macrophages. *Infect. Immun*. **64**, 2765-2773.

Rutherford, A. C., Traer, C., Wassmer, T., Pattni, K., Bujny, M. V., Carlton, J. G., Stenmark, H. and Cullen, P. J. (2006). The mammalian phosphatidylinositol 3-phosphate 5-kinase (PIKfyve) regulates endosome-to-TGN retrograde transport. *J. Cell Sci.* **119**, 3944-3957.

Salcedo, S. P. and Holden, D. W. (2003). SseG, a virulence protein that targets Salmonella to the Golgi network. *EMBO J.* **22**, 5003-5014.

Seaman, M. N. (2004). Cargo-selective endosomal sorting for retrieval to the Golgi requires retromer. *J. Cell Biol*. **165**, 111-122.

Shimada, A., Niwa, H., Tsujita, K., Suetsugu, S., Nitta, K., Hanawa-Suetsugu, K., Akasaka, R., Nishino, Y., Toyama, M., Chen, L. et al. (2007). Curved EFC/F-BAR-domain dimers are joined end to end into filaments for membrane invaginations in endocytosis. *Cell* **129**, 761-772.

Steele-Mortimer, O., Meresse, S., Gorvel, J.-P., Toh, B.-H. and Finlay, B. B. (1999). Biogenesis of Salmonella Typhimurium-containing vacuoles in epithelial cells involves interactions with the early endocytic pathway. *Cell. Microbiol*. **1**, 33-49.

Steele-Mortimer, O., Knodler, L. A., Marcus, S. L., Scheid, M. P., Goh, B., Pfeifer, C. G., Duronio, V. and Finlay, B. B. (2000). Activation of Akt/protein kinase B in epithelial cells by the Salmonella Typhimurium effector SigD. *J. Biol. Chem*. **275**, 37718-37724.

Stein, M. A., Leung, K. Y., Zwick, M., Garcia-del Portillo, F. and Finlay, B. B. (1996). Identification of a Salmonella virulence gene required for formation of filamentous structures containing lysosomal membrane glycoproteins within epithelial cells. *Mol. Microbiol.* **20**, 151-164.

Terebiznik, M. R., Vieira, O. V., Marcus, S. L., Slade, A., Yip, C. M., Trimble, W. S., Meyer, T., Finlay, B. B. and Grinstein, S. (2002). Elimination of host cell PtdIns(4,5)P2 by bacterial SigD promotes membrane fission during invasion by Salmonella. *Nat. Cell Biol*. **4**, 766-773.

Waguri, S., Dewitte, F., Le Borgne, R., Rouille, Y., Uchiyama, Y., Dubremetz, J. F. and Hoflack, B. (2003). Visualization of TGN to endosome trafficking through fluorescently labeled MPR and AP-1 in living cells. *Mol. Biol. Cell* **14**, 142-155.

Wassmer, T., Attar, N., Bujny, M. V., Oakley, J., Traer, C. J. and Cullen, P. J. (2007). A loss-of-function screen reveals SNX5 and SNX6 as potential components of the mammalian retromer. *J. Cell Sci.* **120**, 45-54.

Worby, C. A. and Dixon, J. E. (2002). Sorting out the cellular functions of sorting nexins. *Nat. Rev. Mol. Cell Biol*. **3**, 919-931.

Yip, C. K. and Strynadka, N. C. (2006). New structural insights into the bacterial type III secretion system. *Trends Biochem. Sci*. **31**, 223-230.

Zhong, Q., Lazar, C. S., Tronchere, H., Sato, T., Meerloo, T., Yeo, M., Songyang, Z., Emr, S. D. and Gill, G. N. (2002). Endosomal localization and function of sorting nexin 1. *Proc. Natl. Acad. Sci. USA* **99**, 6767-6772.